Use of time series normalized difference vegetation index (NDVI) to monitor fall armyworm (*Spodoptera frugiperda*) damage on maize production systems in Africa

Marian Adan, Henri E. Z. Tonnang, Klaus Greve, Christian Borgemeister & Georg Goergen

Taylor & Francis
Taylor & Francis Group

Use of time series normalized difference vegetation index (NDVI) to monitor fall armyworm (*Spodoptera frugiperda*) damage on maize production systems in Africa

Marian Adan[a] ⓡ, Henri E. Z. Tonnang[b], Klaus Greve[a] ⓡ, Christian Borgemeister[a] and Georg Goergen[c]

[a]Center for Development Research (ZEF), University of Bonn, Bonn, Germany; [b]International Centre of Insect Physiology and Ecology (ICIPE), Nairobi, Kenya; [c]International Institute of Tropical Agriculture (IITA), Tri Postal, Cotonou, Republic of Benin

ABSTRACT

Fall armyworm (FAW) *Spodoptera frugiperda* (J.E. Smith), damage was monitored at a regional scale using time series data in Western and Southern African countries. The study employed the normalized difference vegetation index (NDVI) computed from Landsat 8 imagery using the Google Earth Engine (GEE) using image composites for the years 2013 to 2020 for the study areas. The index was then reclassified based on the NDVI threshold values into low, sparse, moderate, and dense classes. FAW prevalence data were then utilized to validate the correlation between the FAW infestation and NDVI values. FAW was associated with a decrease in vegetation productivity between the years 2016, 2017, and 2018 when the pest infestation was reported in the study areas. The validation results showed that there is a correlation between FAW infestation and NDVI ($R^2$0.83). Our study highlighted that NDVI can be used as a proxy to quantify pest damage to vegetation productivity.

Introduction

Fall armyworm (FAW), *Spodoptera frugiperda* (J.E. Smith) (Lepidoptera, Noctuidae), is endemic to the Americas, but following its first detection outside of its native range in 2016 (Goergen et al. 2016), it has rapidly spread across different continents (Sharanabasappa et al. 2018; Naeem-Ullah et al. 2019; Sun et al. 2021; IPPC 2022), thereby becoming a true global pest of many important crops, among them chiefly maize and sorghum. Studies have attributed this rapid spread to recent increases in global temperature which provide suitable environmental conditions to the pest (Díaz-Álvarez et al. 2020; Nurzannah et al. 2020). Commonly, FAW thrives under tropical humid conditions to complete its development (Du Plessis et al. 2020). In Africa, the pest was first detected in Nigeria in 2016, followed by São Tomé and Príncipe, Benin, Ghana, Togo and

subsequently also in the Democratic Republic of Congo (DRC) (Goergen et al. 2016). To date FAW has been recorded in 47 out of the 54 African countries (Cabi 2022), driven by the strong dispersal ability of the adult moths which are capable of travelling up to 70 km per day (Ge et al. 2021). In 2018, FAW was first reported in Asia, i.e. India and Yemen, and by 2019 had widely spread with records from China, Malaysia, Indonesia, Pakistan, Japan, South Korea and Australia (Harrison et al. 2019).

Being an invasive species that mostly damages cereal crops, FAW has negatively impacted food and nutrition security, particularly among small scale farmers in Africa (Cock et al. 2017). For instance estimates in 12 African counties indicate that, maize yields have been reduced by 8.3 to 20.6 million tons annually following the FAW invasion (Day et al. 2017). Maize is one of the most important staple food crops in sub-Saharan Africa (SSA), covering approximately 36 million hectares and supporting the livelihoods for about 208 million people on the continent (Day et al. 2017; Assefa and Ayalew 2019). The economic losses by FAW in 12 major maize-growing countries of Africa are estimated at US$2.5 to 6.2 billion (Shylesha et al. 2018).

Earlier studies have demonstrated the use of various geo-spatial and remote sensing tools for effective monitoring of important crop pests like FAW and plant diseases (Acharya and Thapa 2015; Rani et al. 2018; Roberts et al. 2021; Rano et al. 2022). Some of these previous studies predicted habitat suitability of FAW using various modelling approaches at global scale (Tepa-Yotto et al. 2021; Guimapi et al. 2022; Paudel et al. 2022). However, the potential crop damage caused by FAW at finer scales remains to assessed and quantified by means of remote sensing technologies. Remotely sensed data, acquired either with handheld (Filho et al. 2020) or airborne (Bhattarai et al. 2019) sensors, have been used for assessing insect crop damage. Essentially, symptoms of crop damage by insect pests can be visual and/or invisible depending on the attack stage. To develop early warning tools using satellite systems for early insect pest damage detection, there are several sensors such as WorldView-3 that provide imagery of high (<3 m) spatial resolutions. However, to test such operational early warning systems, readily available satellite data should be utilized. Landsat 8, which operates with a multispectral sensor of 30 m spatial resolution, could provide unique data for FAW damage detection at local and regional scales. This could be achieved by integrating Landsat 8 based spectral features and geo-spatial analytics to characterize landscape structure in relation to FAW damage. This approach would enable the assessment of the spatio-temporal FAW damage status in crops like maize and sorghum, which are among the most preferred host plants of the pest (Day et al. 2017). Specifically, time series optical Sentinel-2 spectral bands and vegetation indices can provide a robust, efficient and cost-effective technique for monitoring FAW damage (Horelu et al. 2015; Prabhakar et al. 2020). Though a Sentinel-2 multispectral image has a high spatial resolution of 10 m it's, however, not suitable for long term time series analysis compared to Landsat images due to image availability since the satellite was launched in 2015, hence lacking historical images.

One of the most commonly used differential vegetation index for crop health monitoring is the normalized difference vegetation index (NDVI) (Tucker and Sellers 1986). Generally, NDVI is an indicator of crop vigor, stress and damage as a function of the reflectance at the near infrared (NIR) and red bands (Wall et al. 2008; Huang et al. 2014; Ji et al. 2021). For instance, Prabhakar et al. (2020) used NDVI calculated from Sentinel-2 data to show the viability of site-specific pest management and found that NDVI is quite effective for detecting FAW infestations with an R^2 of 0.80. In another study, Zhang et al. (2016) developed a mapping approach for tracking fall armyworm (FAW) infestation at a regional scale using a univariate model and two-date HJ-CCD (Huanjing satellite charge

coupled device) NDVI. HJ-CCD is also an optical multispectral sensor of 30 m spatial resolution which generates images comparable to Landsat 8, however such images are not available in google earth engine software. This method was found to be effective and promising for use in a typical FAW outbreak event in Tangshan, Hebei Province, China. Furthermore, Zhang et al. (2016) expressed the need for robust and cost-effective remote sensing tools for monitoring FAW damage at a regional scale. Thus, this research aims to create a robust and cost-effective remote sensing instrument for FAW damage on a regional scale in Africa. The study fills the research gap as it utilizes Landsat 8 time series data for pre- and post- FAW invasion period at a regional scale, unlike previous studies that have used Sentinel-2 or other remote sensing technologies for crop damage detection at a site-specific/farm level (Horelu et al. 2015; Prabhakar et al. 2021). The objective of this study is to use multi-date Landsat 8 images and NDVI datasets to evaluate the spatial and temporal status of FAW damage in maize growing areas to cover the pre- and post-FAW infestation to evaluate the pest damage. Additionally, the study seeks to measure the crop damage caused by FAW in both West and South African study areas. The Landsat 8 image was considered for the study due to its narrower spectral bands, improved calibration and signal-to-noise characteristics, higher 12-bit radiometric resolution, and more precise geometry (Roy et al. 2016).

Study area

This study was focused on the following areas: Atlantique region of Benin, Centrale in Togo, Salima in Malawi, Chongwe in Zambia, and Limpopo in South Africa (Figure 1). These study areas were selected based on the presence of maize and sorghum cropping systems (Table 1) in the respective areas and their history of FAW attack. Atlantique is one of the 12 departments in Benin, located between latitude 6° 20′ 00″ N to 6° 50′ 00″ N and longitude 2° 0′ 00″ E to 2° 20′ 00″ E in the south of the country. It covers an area
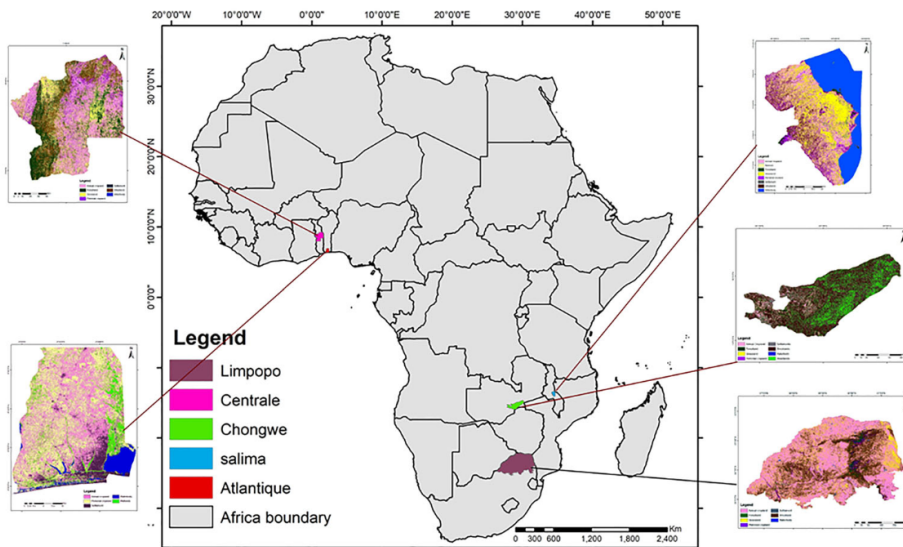

Figure 1. Study area map showing the study regions located in western and southern Africa: Centrale (Togo), Atlantique (Benin), Salima (Malawi), Chongwe (Zambia), and Limpopo (South Africa).

Table 1. Cropping Surface of Maize and Sorghum for the study area in hectares (ha).

Region, Country	Maize cropping surface ha	Sorghum cropping surface ha
Atlantique, Benin	19,000	7,000
Centrale, Togo	28,000	9,000
Salima, Malawi	43,000	6,400
Chongwe region in Zambia	19,000	6,900
Limpopo, South Africa	464,000	16,000

Source: FAO 2018. Statistical yearbook 2018. Retrieved from http://www.fao.org/state-of-food-security-nutrition/en/

of 3,233 km^2 with an estimated population of 1.397 million, annual precipitation of 1,200mm and an annual temperature range between 28° and 32 °C. Approximately 60% of its population depend on agriculture for food and income (Atindogbe et al. 2012).

The Centrale region of Togo is located between latitude 8° 0′ 00″N to 9° 0′ 00″N and longitude 1° 0′ 00″ E to 1° 0′ 00″ E with an area of 13,420 km^2, annual rainfall between 1,200-1,500mm and an annual temperature range between 20° and 39 °C. The main economic activity within the study site is agriculture with a population totaling 617,871 as of the 2010 census (Ataba et al. 2020). The Salima district of Malawi is located between latitude 13° 30′ 00″ S to 14° 0′ 00″ S and longitude 34° 10′ 00″ E to 34° 40′ 00″ E, covers an area of 2,196 km^2, with a population of 478,368 (Government of Malawi, 2018), and a mean annual precipitation of 1,188mm as unimodal rainfall. With an average annual temperature of 22 °C, the district has a tropical climate. The district is dominated by small holder agriculture, covering approximately 107,400 hectares (Musa et al. 2018).

The Chongwe district in the Lusaka province of Zambia is located between latitude 15° 0′ 00″ S to 16° 0′ 00″ S and longitude 28° 0′ 00″ E to 30° 0′ 00″ E, covers an area of 8,669 km^2, with a population of 192,303, and precipitation ranges between 800-1,000mm with an annual temperature of 20.4 °C (Jacqueline and Mubanga 2020) . Agriculture is the most important economic activity, primarily with crops like maize, cassava, and sweet potatoes (CSO, 2003). Finally, the Limpopo Province of South Africa lies between latitude 23° 0′ 00″ S to 25° 0′ 00″ S and longitude 27° 0′ 00″ E to 31° 0′ 00″ E, covering an area of 125,754 km^2, an estimated population of 5,778,400, an annual temperature ranging between 24.6 − 28.2 °C, 500 mm of total annual rainfall, with commercial farmers occupying >70% of the province's prime agricultural land, while smallholder farmers occupying the remaining arable surface (Cai et al. 2017).

Methodology

Data description

Landsat 8 satellite data

Landsat 8 multispectral top of the atmosphere images (LANDSAT/LC08/C01/T1_TOA) were utilized for the analysis. The Landsat 8 has a spatial resolution of 30 m with 11 spectral bands distributed between the visible, near-infrared (NIR), shortwave infrared (SWIR) and thermal infrared (TIRS) regions of the electromagnetic spectrum (EMS). The sensor has an altitude of 705 km and a temporal resolution (revisit time) of 16 days (USGS, 2021).

Data analysis

The methodology framework of this study consisted of four main steps (Figure 2).
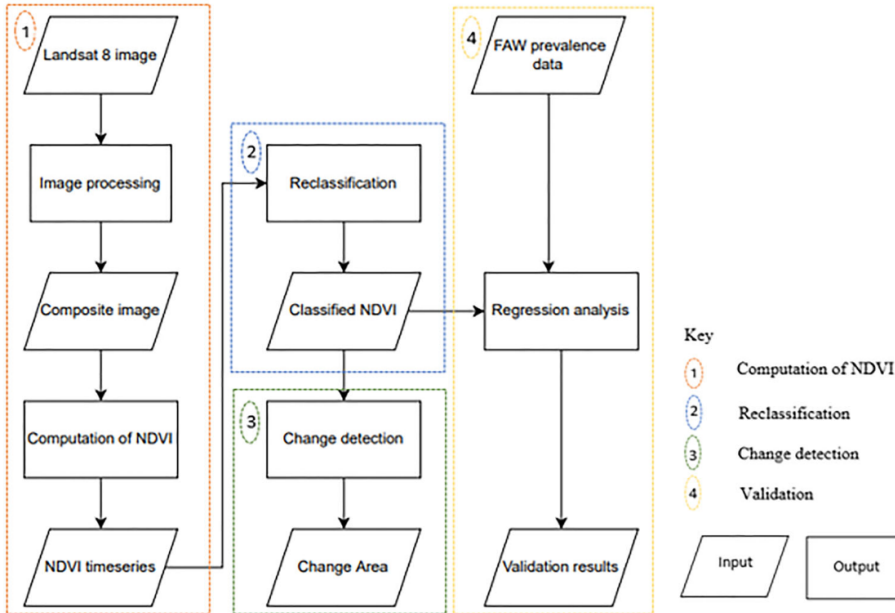
Figure 2. Flowchart of the hierarchical methodology steps for assessing and quantifying the damage of fall army-worm on maize productivity using the normalized difference vegetation index (NDVI).

Table 2. Landsat 8 satellite images 11 spectral bands, which are used to capture different aspects of the Earth's surface.

Band Number	Band Name	Wavelength (μm)	Resolution (m)
1	Coastal	0.44 − 0.48	30
2	Blue	0.45 − 0.51	30
3	Green	0.53 − 0.59	30
4	Red	0.64 − 0.67	30
5	NIR1	0.84 − 0.88	30
6	SWIR1	1.57 − 1.65	30
7	SWIR2	2.11 − 2.29	30
8	Panchromatic	0.50 − 0.68	15
9	Cirrus	1.36 − 1.38	30

Table 2 lists the spectral bands of a satellite sensor, along with their band numbers, names, wavelength ranges in micrometers (μm), and spatial resolutions in meters. The sensor has eight multispectral bands (bands 1-7 and 9) and one panchromatic band (band 8). The multispectral bands cover a wide range of wavelengths from the visible to the near-infrared (NIR) and shortwave infrared (SWIR) regions of the electromagnetic spectrum. The spatial resolution of the multispectral bands is 30 meters, while the panchromatic band has a higher resolution of 15 meters. Additionally, the sensor has a Cirrus band (band 9) that is sensitive to high-altitude clouds.

Step 1: Landsat 8 (Table 2) images were obtained and processed using Google Earth Engine (GEE) software (https://code.earthengine.google.com), which is a cloud computing software (Kumar and Mutanga 2018). The image processing involved cloud masking of which band quality band (BQA) was utilized, also atmospheric correction was utilized to remove the effects of atmospheric scattering and absorption on the images, as these factors can affect the NDVI values. A total of 415, 613, 909, 320, and 517 images were used for the Atlantique, Centrale, Chongwe, Salima, and Limpopo regions, respectively.

A composite image was then computed using the median values of the pixels for each year, covering the months January to December of 2013 to 2020 for the selected study

regions to compute the NDVI using the Red (band 4) and NIR (band 5) bands (Table 1) of Landsat images (Equation 1).

$$\text{NDVI} = \frac{(NIR - Red)}{(NIR + Red)} \qquad \text{(Equation 1).}$$

where NIR and red are reflectance values at near-infrared and red bands 5 and 4 of Landsat 8, respectively.

Step 2: The NDVI values were reclassified into four classes, i.e. Low, sparse, moderate, and dense vegetation, using the reclassify tool in QGIS (QGIS.org, QGIS 2020) to quantify FAW crop damage in terms of vegetation change. The sparse and moderate vegetation productivity comprised of bare soil and grassland classes, while the dense vegetation entailed annual cropland, perennial cropland, forestland and woodlands (Akbar et al. 2019). The natural breaks threshold technique (Singh and Javeed 2021) was then used to reclassify the NDVI values into the four vegetation classes. The method was used to find class breaks that best group standard deviation data with comparable values while also maximizing the difference between classes (Table 3).

The NDVI threshold values listed for each vegetation class in the study regions are based on empirical observations and previous research. NDVI values provide an estimation of vegetation density and vigor, with higher values indicating denser and healthier vegetation cover. The threshold values are used to classify different vegetation classes based on their NDVI ranges. These values can vary depending on the specific region, climate, and vegetation types. Therefore, the values listed for each study region and vegetation class have been determined through previous research and field observations to best fit the local vegetation patterns and characteristics (Singh and Javeed 2021).

Step 3: The specific year of which the FAW was identified for each study site was obtained from literature. (Goergen et al. 2016; Koffi et al. 2020; Dassou et al. 2021). The vegetation density class for each study region for the period before and after the

Table 3. The threshold range of the normalized difference vegetation index (NDVI) values for the four vegetation density classes viz., water body, low, sparse, moderate, and dense vegetation for the five study regions.

Study region	Vegetation class	NDVI values range
Atlantique (Benin)	Low vegetation	−0.15 to 0.10
	Sparse vegetation	0.10 to 0.26
	Moderate vegetation	0.26 to 0.36
	Dense vegetation	0.36 to 0.67
Centrale (Togo)	Low vegetation	−0.10 to 0.39
	Sparse vegetation	0.36 to 0.47
	Moderate vegetation	0.47 to 0.54
	Dense vegetation	0.54 to 0.77
Salima (Malawi)	Low vegetation	−0.48 to −0.04
	Sparse vegetation	−0.04 to 0.22
	Moderate vegetation	0.22 to 0.31
	Dense vegetation	0.31 to 0.75
Chongwe (Zambia)	Low vegetation	−0.37 to 0.05
	Sparse vegetation	0.05 to 0.28
	Moderate vegetation	0.28 to 0.36
	Dense vegetation	0.36 to 0.77
Limpopo (South Africa)	Low vegetation	−0.67 to −0.00
	Sparse vegetation	−0.00 to 0.27
	Moderate vegetation	0.27 to 0.41
	Dense vegetation	0.41 to 0.84

The range of NDVI values for each vegetation class in five different study regions in table 3: Atlantique (Benin), Centrale (Togo), Salima (Malawi), Chongwe (Zambia), and Limpopo (South Africa). The Low vegetation class had the lowest NDVI values, ranging from -0.67 to -0.04, while the Dense vegetation class had the highest values, ranging from 0.31 to 0.84. The range of NDVI values for Sparse vegetation and Moderate vegetation classes varied between regions.

introduction of FAW was then computed using mulusce plugins in QGIS software, an algorithm subtracting annual NDVI values for pre and post FAW infestation expressed in hectares. The 2013 annual average NDVI values were used as a reference to quantify subsequent crop damage, since it was a year with high NDVI values in many of the study regions during pre-FAW introduction.

Step 4: The validation data were obtained from the Food and Agricultural Organization of the United Nations (FAO) collected in the selected study sites across Africa (FAO 2018). We utilized FAW data for the year 2018/2019 (January – December) for which geographic location together with field collected information about different crop types were available. Hence, the points were filtered to focus on maize farm field samples. The original excel data were then converted into a shapefile in QGIS software. The field data points were later overlaid on the NDVI raster data sets, of which the NDVI values were extracted for each point of FAW prevalence, using the extract values by points tool in QGIS. Linear regression was then applied to validate the correlation between NDVI values and the prevalence of FAW that was computed using the scouting data obtained from the field that signified the presence of FAW by rating the proportion of plants affected by the pest.

Results

NDVI classification

Figure 3 highlights the variation in the classified NDVI images. In Atlantique, Benin (Figure 3a), there was a higher sparse and moderate vegetation density in 2013 than the densely vegetated class in 2016. In the other years, there was no consistent overall trend in vegetation density with the dense vegetation class more dominant in the region in 2014 and 2019. In the Centrale region of Togo (Figure 3b), the density of vegetation was decreasing over the years with density values in 2013 being considerably higher than in 2020. In Salima, Malawi (Figure 3c), the vegetation density was lower in 2017 than in 2013. A similar trend was observed in Limpopo (South Africa) (Figure 3d), and also in Chongwe (Zambia) (Figure 3e), the vegetation cover in 2018 was lower than in 2013.

Average annual NDVI time-series

In 2016, the variation in the yearly average NDVI for Atlantique (a) and Centrale (b) was minimal in both areas, as seen in Figure 4 The lowest average NDVI for Chongwe (c) was reported in 2014, then climbed in 2015 before continuing to decline until 2020. The lowest NDVI values were recorded in Salima (d) and Limpopo (e) in 2017 and 2018, respectively.

Area of change for the NDVI classes

We observed a decrease in moderate and dense vegetation classes by 4% and 19%, respectively, for the Atlantique (Benin) and Centrale (Togo) regions in 2016, and for the latter country also an increase in sparse (4%) and low vegetation (19%) (Tables 4 and 5). For Chongwe (Zambia) and Salima (Malawi) we noted a decrease in moderate and dense vegetation classes (Tables 6 and 7), and for Limpopo (South Africa) a decrease in dense, moderate and sparse vegetation between 2013 and 2018 (Table 8).
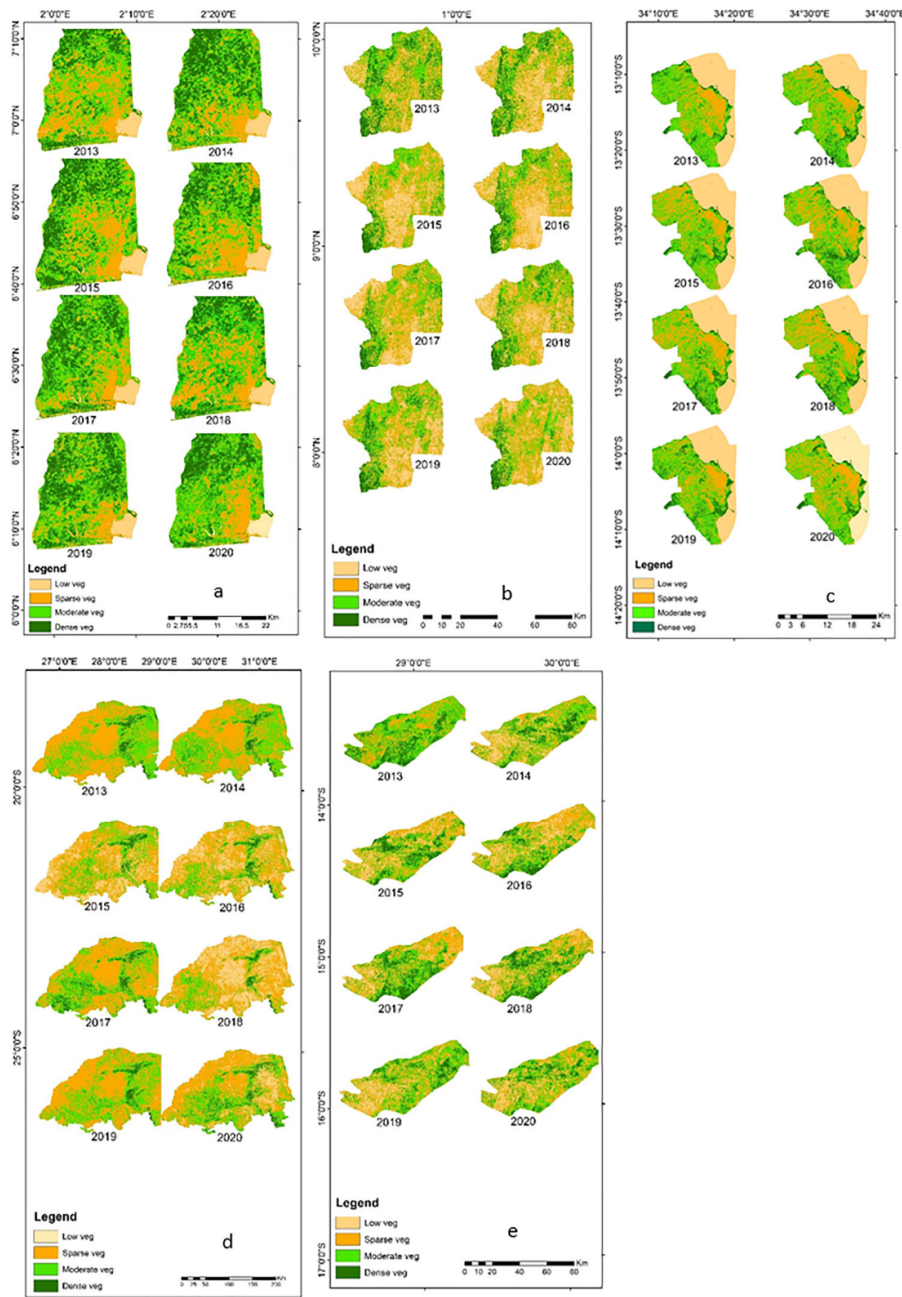
Figure 3. The classified normalized difference vegetation index (NDVI) for the years 2013 to 2020, for the regions of a) Atlantique (Benin), b) Centrale (Togo), c) Salima (Malawi), d) Limpopo (South Africa) and e) Chongwe (Zambia).
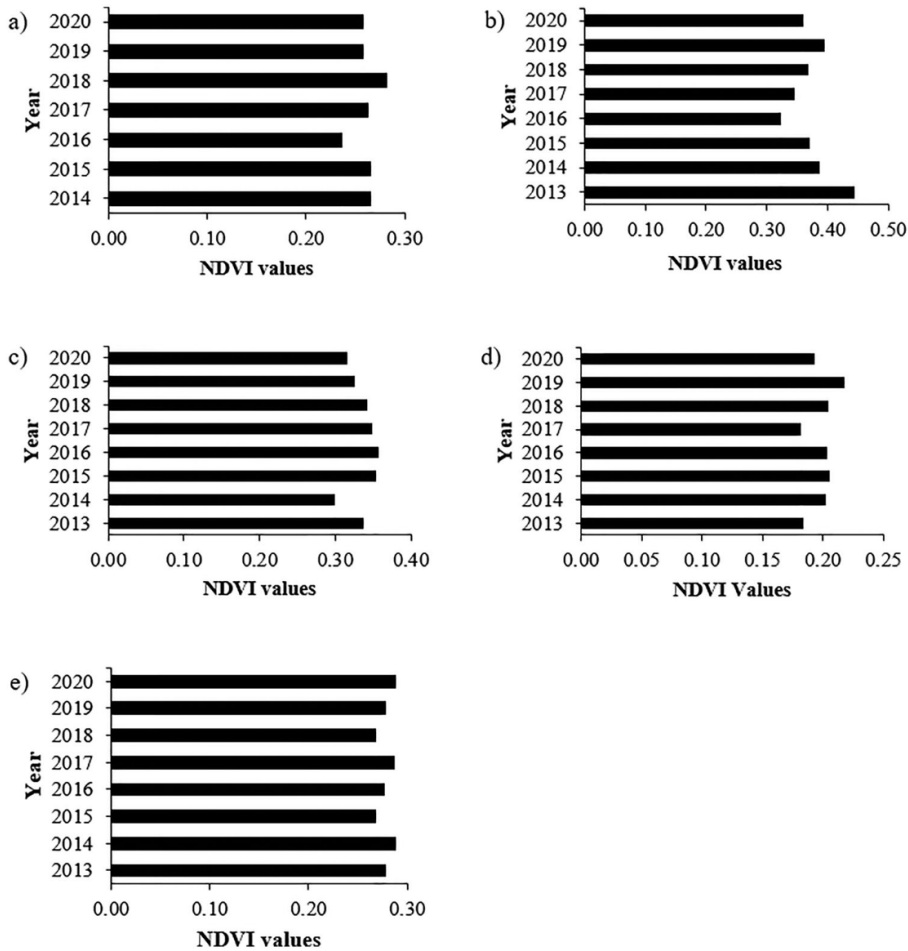
Figure 4. Annual average normalized difference vegetation indices (NDVI) from 2013 to 2020 for the regions of a) Atlantique (Benin), b) Centrale (Togo), c) Chongwe (Zambia), d) Salima (Malawi), and e) Limpopo (South Africa).

Table 4. Area and percentage of change in the normalized difference vegetation index (NDVI) classes between 2013 and 2016 for the Atlantique region of Benin (veg. = vegetation).

| NDVI class | Area (ha) | | Difference (ha) | Change (%) | | Difference (%) |
	2013	2016	Δ	2013	2016	Δ
Low veg.	14931.99	15647.91	715.92	4.86	5.09	0.23
Sparse veg.	94165.94	104702.21	10536.28	30.65	34.08	3.43
Moderate veg.	127876.97	126585.90	−1291.08	41.62	41.20	−0.42
Dense veg.	70267.69	60306.57	−9961.12	22.87	19.63	−3.24

Difference (ha) and Change (%) columns in the table 4 shows the change in area and percentage change, respectively, for each vegetation class between 2013 and 2016. A positive or negative sign indicates whether the area increased or decreased, respectively.

Validation

There was a significant (P, 0.05) positive correlation between the NDVI values and FAW prevalence with a strong R^2 of 0.83 (Figure 5), implying a higher FAW prevalence with lower NDVI values and vice versa.

Table 5. Area and percentage of change for the normalized difference vegetation index (NDVI) classes between 2013 and 2016 for the Centrale region of Togo (veg. = vegetation).

NDVI class	Area (ha)		Difference (ha)	Change (%)		Difference (%)
	2013	2016	Δ	2013	2016	Δ
Low veg.	165432.06	358454.01	193021.95	12.49	27.05	14.57
Sparse veg.	431605.47	491854.69	60249.22	32.58	37.12	4.55
Moderate veg	484141.68	342134.53	−142007.15	36.54	25.82	−10.71
Dense veg.	243706.11	132442.09	−111264.02	18.40	1.00	−8.40

Difference (ha) and Change (%) columns in the table 5 shows the change in area and percentage change, respectively, for each vegetation class between 2013 and 2016. A positive or negative sign indicates whether the area increased or decreased, respectively.

Table 6. Area and percentage of change for the normalized difference vegetation index (NDVI) classes between 2013 and 2017 for the Chongwe region of Zambia (veg. = vegetation).

NDVI Class	Area (ha)		Difference (ha)	Change (%)		Difference (%)
	2013	2017	Δ	2013	2017	Δ
Low veg.	266.85	200410.83	200143.98	18.43	18.41	0.02
Sparse veg.	313848.90	429315.49	115466.59	28.87	39.50	10.60
Moderate veg.	539585.67	317554.72	−222029.95	49.64	29.20	−20.40
Dense veg.	233235.93	139655.31	−93580.62	21.46	12.85	−8.61

Difference (ha) and Change (%) columns in the table 6 shows the change in area and percentage change, respectively, for each vegetation class between 2013 and 2017. A positive or negative sign indicates whether the area increased or decreased, respectively.

Table 7. Area and percentage of change for the normalized difference vegetation index (NDVI) classes between 2013 and 2017 for the Salima region of Malawi (veg. = vegetation).

NDVI Class	Area (ha)		Difference (ha)	Change (%)		Difference (%)
	2013	2017	Δ	2013	2017	Δ
Low veg.	97298.64	96534.19	−764.45	31.18	30.93	−0.24
Sparse veg.	65001.06	105596.58	40595.52	20.83	33.83	13.00
Moderate veg.	108690.06	93423.57	−15266.48	34.83	29.93	−4.89
Dense veg.	41105.16	16540.58	−24564.58	13.17	5.30	−7.87

Difference (ha) and Change (%) columns in the table 7 shows the change in area and percentage change, respectively, for each vegetation class between 2013 and 2017. A positive or negative sign indicates whether the area increased or decreased, respectively.

Table 8. Area and percentage of change for the normalized difference vegetation index (NDVI) classes between 2013 and 2018 for Limpopo, South Africa (veg = vegetation).

NDVI class	Area (ha)		Difference (ha)	Change (%)		Difference (%)
	2013	2018	Δ	2013	2018	Δ
Low veg.	21195.16	4195000.91	4173805.75	0.17	34.02	33.85
Sparse veg.	6854595.74	5769171.76	−1085423.99	55.59	46.78	−8.80
Moderate veg.	4776531.85	1999759.36	−2776772.49	38.73	16.22	−22.51
Dense veg.	679377.82	367768.54	−311609.28	5.51	2.98	−2.53

Difference (ha) and Change (%) columns in the table 8 shows the change in area and percentage change, respectively, for each vegetation class between 2013 and 2018. A positive or negative sign indicates whether the area increased or decreased, respectively.

Discussion

The study could conclusively show that NDVI can be used as a proxy for monitoring FAW induced crop damage. With multi-date NDVI data we could detect changes in vegetation density from before to after the FAW invasion in the study regions. For each of
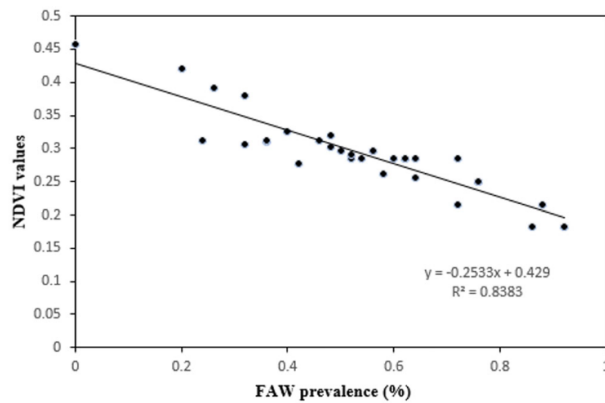
Figure 5. Correlation between the normalized difference vegetation index (NDVI) and prevalence of fall armyworm (FAW) in five regions of sub-Saharan Africa, i.e. the regions of a) Atlantique (Benin), b) Centrale (Togo), c) Chongwe (Zambia), d) Salima (Malawi), and e) Limpopo (South Africa).

the latter, we used the year 2013 as the pre-FAW infestation reference year and hypothesized that after FAW was introduced, i.e. 2016 for Benin and Togo, 2017 for Malawi and Zambia, and 2018 for South Africa, drops in NDVI could be attributed to the impact of the pest (Goergen et al. 2016; Abrahams et al. 2017; Murray et al. 2019; Koffi et al. 2020; Dassou et al. 2021; Kasoma et al. 2021). This is consistent with other studies that utilized spectral vegetation indices such as NDVI to monitor crop health and vigor (Wall et al. 2008; Huang et al. 2014; Ji et al. 2021). For instance, Prabhakar et al. (2020) used NDVI to detect FAW damage in sorghum. The authors utilized Sentinel-2 derived NDVI to detect FAW infestation at farm level in southern India, and could correlate pest infestation with NDVI at an R^2 of 0.80 very similar to the R^2 0.83 in our study. Like other noctuid pests, FAW damages maize and sorghum crops and cause defoliation and stem damage, resulting in substantial yield losses (FAO 2018). These crop morphological and physiological symptoms can cause considerable changes in the crop spectral features, particularly in the red and NIR portions of the EMS. The red and NIR portion of the EMS, which is used to calculate the NDVI, are known chlorophyl and water sensitive features that can mimic the changes in the crop chlorophyl and water content due to pest damage (Yamanura and Patil 2021).

In Zambia, a 40% decline in NDVI magnitude was reported during the 2016/2017 cropping season and continued to decline until 2018 (Kansiime et al. 2019). This is corroborated with our findings, which show that the frequency of NDVI values decreased from 2017 to 2020. It is highly likely, that the massive FAW outbreaks in 2016/2017 in Zambia, with >124,000 ha of maize affected, could have been the reason for the observed NDVI reductions (Kansiime et al. 2019). Also, the level of NDVI reductions can vary depending on the FAW intervention measures applied. For instance, in Zambia, the NDVI values continued to decline following the 2016 invasion until 2020, possibly because of shortcomings in information dissemination to affected farmers, and inadequate control methods coupled with a lack of reliable access to insecticides (Kasoma et al. 2021). Yet, in countries like Benin, Togo, and Malawi, NDVI values increased after the FAW invasion, possibly because of more successful pest control intervention utilizing synthetic and biological insecticides which led to a considerable drop in FAW population levels (CABI 2018). Similar

observations were made in Togo, with FAW levels decreasing from 68.5% to 55.8% and 17.8% in 2016, 2017, and 2018, respectively, due to the increased use of synthetic insecticides (Koffi et al. 2020).

Nonetheless, it is worth noting that NDVI is not only affected by insect pest damages but also by other biotic and abiotic factors such as crop diseases, weeds, drought, flood, nutrient deficiencies etc. (Pei et al. 2019). For instance, the NDVI decrease in Chongwe (Zambia) and Limpopo (South Africa) in 2014 and 2015 prior to the FAW invasion were a result of El Niño oscillations (Archer et al. 2017). Moreover, the region experienced a severe drought from 2014 to 2015, which caused a considerable reduction in NDVI and crop yield (Liu and Zhou 2021). However, the effect of precipitation on NDVI cannot be confounded with other biotic and abiotic factors as the index steadily increases if rainfall is abundant and vice versa (Pei et al. 2019; Achille et al. 2021). Also, the impact of temperature changes on NDVI is minimal (Wang et al. 2003).

Conclusions

Our study demonstrates that NDVI can be utilized as a proxy for monitoring crop damage caused by FAW. Essentially, the study reclassified NDVI imagery to four greenness classes viz., low, sparse, moderate and dense vegetation, to quantify crop damage due to FAW infestation. The study hypothesized that the change in NDVI between 2013, 2014, 2015 (pre FAW invasion), and 2016, 2017 and 2018 (post FAW invasion) were caused by FAW damage. We found considerable reductions in NDVI in all study regions of Benin, Togo, Malawi, Zambia and South Africa post FAW invasion. Our results can be used as a guide for monitoring the effectiveness of pest control methods that are currently rolled out across Africa to mitigate FAW effects on important staple crops like maize and sorghum. They can also be used to estimate crop yield as a function of FAW damage in affected regions. Finally, we believe that future studies should look at testing our approach in other FAW affected regions of SSA and field validated with data on FAW damage and yield.

Disclosure statement

No potential conflict of interest was reported by the authors.

Author's contribution

Marian Adan: methodology, formal analysis, visualization, data curation, and writing. **Henri E. Z. Tonnang:** conceptualization, supervision, data curation, review, and funding acquisition. **Klaus Greve:** methodology, review and editing. **Christian Borgemeister:** conceptualization, methodology, review, editing, and funding acquisition. **Georg Goergen:** conceptualization, methodology, review, editing, and funding acquisition. All authors have read and agreed to the content of the manuscript.

Zentrum für Entwicklungsforschung (ZEF), Bonn, Germany. It has been carried out in partial fulfillment of a Ph.D. thesis by the first author in close collaboration with the International Centre of Insect Physiology and Ecology (*icipe*) Nairobi, Kenya, and the International Institute of Tropical Agriculture (IITA) Cotonou, Benin.

ORCID

Marian Adan http://orcid.org/0000-0003-3808-9920
Klaus Greve http://orcid.org/0000-0001-6463-6161

Data availability statement

The datasets generated during and/or analyzed during the current study are available from the corresponding author upon reasonable request.

References

Abrahams P, Bateman M, Beale T, Clottey V, Cock M, Colmenarez Y, Corniani N, Day R, Early R, Godwin J, et al. 2017. Fall Armyworm: impacts and implications for Africa. Evidence Note. 2:144. September 2017. Report to DFID.Center for Agriculture and Bioscience International-CABI (2017).

Acharya MC, Thapa RB. 2015. Remote sensing and its application in agricultural pest management. J Agric & Environ. 16:43–61.

Achille LS, Zhang K, Anoma CJK. 2021. Analysis of climate variability and relation to vegetation in Garamba National Park from 1990-2020. OJE. 11(10):700–723.

Akbar TA, Hassan QK, Ishaq S, Batool M, Butt HJ, Jabbar H. 2019. Investigative spatial distribution and modelling of existing and future urban land changes and its impact on urbanization and economy. Remote Sens. 11(2):105.

Archer ERM, Landman WA, Tadross MA, Malherbe J, Weepener H, Maluleke P, Marumbwa FM. 2017. Understanding the evolution of the 2014–2016 summer rainfall seasons in Southern Africa: key lessons. Clim Risk Manag. 16:22–28.

Assefa F, Ayalew D. 2019. Status and control measures of fall armyworm (*Spodoptera frugiperda*) infestations in maize fields in Ethiopia: a review. Cogent Food Agric. 5(1):1641902.

Ataba E, Katawa G, Ritter M, Ameyapoh AH, Anani K, Amessoudji OM, Tchadié PE, Tchacondo T, Batawila K, Ameyapoh Y, et al. 2020. Ethnobotanical survey, anthelmintic effects and cytotoxicity of plants used for treatment of helminthiasis in the Central and Kara regions of Togo. BMC Complement Altern Med. 20(1):212.

Atindogbe G, Fonton NH, Fandohan AB, Lejeune P, Fonton H, Fandohan B. 2012. Characterization of private teak (*Tectona grandis L.f.*) plantations in the Atlantic Department of South Benin. In Biotechnol Agron Soc Environ. 16(4):441–451.

Bhattarai GP, Schmid RB, McCornack BP. 2019. Remote sensing data to detect hessian fly infestation in commercial wheat fields. Sci Rep. 9(1):1–11.

Cabi. 2022. *Spodoptera frugiperda* (fall armyworm) datasheet. Crop protection compendium. [accessed 2022 May 17]. https://www.cabi.org/cpc/datasheet/29810#todistributionDatabaseTable.

Cai X, Magidi J, Nhamo L, van Koppen B. 2017. Mapping irrigated areas in the Limpopo Province, South Africa. Vol. 172. International Water Management Institute (IWMI).

Cock MJ, Beseh PK, Buddie AG, Cafá G, Crozier J. 2017. Molecular methods to detect *Spodoptera frugiperda* in Ghana, and implications for monitoring the spread of invasive species in developing countries. Sci Rep. 7(1):1–10.

Dassou AG, Idohou R, Azandémè-Hounmalon GY, Sabi-Sabi A, Houndété J, Silvie P, Dansi A. 2021. Fall armyworm, *Spodoptera frugiperda* (JE Smith) in maize cropping systems in Benin: abundance, damage, predatory ants and potential control. Int J Trop Insect Sci. 41(4):2627–2636.

Day R, Abrahams P, Bateman M, Beale T, Clottey V, Cock M, Colmenarez Y, Corniani N, Early R, Godwin J, et al. 2017. Fall armyworm: impacts and implications for Africa. Outlook Pest Man. 28(5): 196–201.

Díaz-Álvarez EA, Martínez-Zavaleta JP, López-Santiz EE, de la Barrera E, Larsen J, del-Val E. 2020. Climate change can trigger fall armyworm outbreaks: a developmental response experiment with two Mexican maize landraces. Int J Pest Manag.66(4): 265-273

Du Plessis H, Schlemmer ML, Van den Berg J. 2020. The effect of temperature on the development of *Spodoptera frugiperda* (Lepidoptera: Noctuidae). Insects. 11(4):228.

FAO. 2018. Integrated management of the Fall Armyworm on maize A guide for Farmer Field Schools in Africa; p. 119.

Filho FH, Heldens WB, Kong Z, de Lange ES. 2020. Drones: innovative technology for use in precision pest management. J Econ Entomol. 113(1):1–25.

Ge SS, He LM, He W, Yan R, Wyckhuys KA, Wu KM. 2021. Laboratory-based flight performance of the fall armyworm, *Spodoptera frugiperda*. J Integr Agric. 20(3):707–714.

Goergen G, Kumar PL, Sankung SB, Togola A, Tam M. 2016. First report of outbreaks of the fall armyworm *Spodoptera frugiperda* (J E Smith) (Lepidoptera, Noctuidae), a new alien invasive pest in West and Central Africa. PLoS One. 11(10):e0165632.

Guimapi RA, Niassy S, Mudereri BT, Abdel-Rahman EM, Tepa-Yotto GT, Subramanian S, Mohamed SA, Thunes KH, Kimathi E, Agboka KM, et al. 2022. Harnessing data science to improve integrated management of invasive pest species across Africa: an application to Fall armyworm (*Spodoptera frugiperda*) (JE Smith) (Lepidoptera: noctuidae. GECCO. 35(2022):e02056.

Harrison RD, Thierfelder C, Baudron F, Chinwada P, Midega C, Schaffner U, van den Berg J. 2019. Agro-ecological options for fall armyworm (*Spodoptera frugiperda)* (JE Smith) management : Providing low-cost, smallholder friendly solutions to an invasive pest. J Environ Manage. 243:318–330.

Horelu A, Leordeanu C, Apostol E, Huru D, Mocanu M, Cristea V. 2015. Forecasting techniques for time series from sensor data. In: 2015 17th international symposium on symbolic and numeric algorithms for scientific computing (SYNASC);Timisoara, Romania. p. 261–264.

Huang J, Wang H, Dai Q, Han D. 2014. Analysis of NDVI data for crop identification and yield estimation. IEEE J Sel Top Appl Earth Observations Remote Sens. 7(11):4374–4384.

IPPC. 2022. Official pest reports. [accessed 2022 May 17]. https://www.ippc.int/en/countries/all/pestreport.

Jacqueline M, Mubanga KH. 2020. Smallholder farmer's livelihood diversification as a response to changed climatic patterns in Chongwe district, Zambia. JAP. 3(1):1–17.

Ji Z, Pan Y, Zhu X, Wang J, Li Q. 2021. Prediction of crop yield using phenological information extracted from remote sensing vegetation index. Sensors. 21(4):1406.

Kansiime MK, Mugambi I, Rwomushana I, Nunda W, Lamontagne-Godwin J, Rware H, Phiri NA, Chipabika G, Ndlovu M, Day R. 2019. Farmer perception of fall armyworm (*Spodoptera frugiderda* J.E. Smith) and farm-level management practices in Zambia. Pest Manag Sci. 75(10):2840–2850.

Kasoma C, Shimelis H, Laing MD, Shayanowako A, Mathew I. 2021. Outbreaks of the fall armyworm (*Spodoptera frugiperda*), and maize production constraints in Zambia with special emphasis on coping strategies. Sustainability. 13(19):10771.

Koffi D, Agboka K, Adenka DK, Osae M, Tounou AK, Anani Adjevi MK, Fening KO, Fening KO, Meagher RL. 2020. Maize Infestation of fall armyworm (Lepidoptera: noctuidae) within agro-ecological zones of Togo and Ghana in West Africa 3 yr after Its Invasion. Environ Entomol. 49(3):645–650.

Kumar L, Mutanga O. 2018. Google Earth Engine applications since inception: usage, trends, and potential. Remote Sens. 10(10):1509.

Liu X, Zhou J. 2021. Assessment of the continuous extreme drought events in Namibia during the last decade. Water. 13(20):2942.

Murray K, Jepson PC, Chaola M. 2019. Fall armyworm management by maize smallholders in Malawi: an integrated pest management strategic plan. [accessed 2022 March 10]. https://repository.cimmyt.org/bitstream/handle/10883/20170/60695.pdf?sequence=1&isAllowed=y.

Musa FB, Kamoto JF, Jumbe CB, Zulu LC. 2018. Adoption and the role of fertilizer trees and shrubs as a climate smart agriculture practice: the case of Salima District in Malawi. Environments. 5(11):122.

Naeem-Ullah U, Ashraf MA, Iqbal N, Saeed S. 2019. First authentic report of *Spodoptera frugiperda* (JE Smith) (Noctuidae: lepidoptera) an alien invasive species from Pakistan. ASBE. 6:1–3.

Nurzannah SE, Girsang SS, Girsang MA, Effendi R. 2020. Impact of climate change to fall armyworm attack on maize in Karo District, North Sumatera. IOP Conference Series: earth Environ Sci. 484(1): 1–8.

Paudel TB, Niassy S, Kimathi E, Abdel-Rahman EM, Seidl-Adams I, Wamalwa M, Tonnang HE, Ekesi S, Hughes DP, Rajotte EG, et al. 2022. Potential distribution of fall armyworm in Africa and beyond, considering climate change and irrigation patterns. Sci Rep. 12(1):1–15.

Pei Z, Fang S, Yang W, Wang L, Wu M, Zhang Q, Han W, Khoi DN. 2019. The relationship between NDVI and climate factors at different monthly time scales: a case study of grasslands in inner mongolia, China (1982-2015. Sustainability. 11(24):7243.

Prabhakar M, Gopinath KA, Kumar NR, Thirupathi M, Sravan US, Kumar GS, Siva GS, Meghalakshmi G, Vennila S. 2020. Detecting the invasive fall armyworm pest incidence in farm fields of southern India using Sentinel-2A satellite data. Geocarto Int.37:13,3801-3816..

QGIS. 2020. Qgis Geographic Information System 2020. Open source geospatial foundation project. [accessed 2020 September 4]. http://qgis.org.

Rani DS, Venkatesh MN, SriCh NS, Kumar KA. 2018. Remote sensing as pest forecasting model in agriculture. Int J Curr Microbiol Appl Sci. 7(3):280–2689.

Rano SH, Afroz M, Rahman MM. 2022. Application of GIS on monitoring agricultural insect pests: a review.RFNA.3(1): 19–23.

Roberts DP, Short NM, Sill J, Lakshman DK, Hu X, Buser M. 2021. Precision agriculture and geospatial techniques for sustainable disease control. Indian Phytopathol. 74(2):287–305.

Roy DP, Kovalskyy V, Zhang HK, Vermote EF, Yan L, Kumar SS, Egorov A. 2016. Characterization of Landsat-7 to Landsat-8 reflective wavelength and normalized difference vegetation index continuity. Remote Sens Environ. 185:57–70.

Sharanabasappa, Kalleshwaraswamy CM, Asokan R, Swamy HM, Maruthi MS, Pavithra HB, Hegde K, Navi S, Prabhu ST, Goergen G. 2018. First report of the fall armyworm, *Spodoptera frugiperda* (JE Smith) (Lepidoptera: Noctuidae), an alien invasive pest on maize in India. Pest Manage Hortic Ecsyst. 24:23–29.

Shylesha AN, Jalali SK, Gupta A, Varshney R, Venkatesan T, Shetty P, Ojha R, Ganiger PC, Navik O, Subaharan K, et al. 2018. Studies on new invasive pest *Spodoptera frugiperda* (JE Smith) (Lepidoptera: Noctuidae) and its natural enemies. Biol Control. 32(3):145–151.

Singh P, Javeed O. 2021. NDVI based assessment of land cover changes using remote sensing and GIS (A case study of Srinagar district, Kashmir). SAFER. 9(4):491-504

Sun X, Hu C, Jia H, Wu Q, Shen X, Zhao S, Jiang Y, Wu K. 2021. Case study on the first immigration of fall armyworm, *Spodoptera frugiperda* invading into China. J Integr Agric. 20(3):664–672.

Tepa-Yotto GT, Tonnang HE, Goergen G, Subramanian S, Kimathi E, Abdel-Rahman EM, Flø D, Thunes KH, Fiaboe KK, Niassy S, et al. 2021. Global habitat suitability of *Spodoptera frugiperda* (JE Smith) (Lepidoptera, Noctuidae): Key parasitoids considered for its biological control. Insects. 12(4):273.

Tucker CJ, Sellers PJ. 1986. Satellite remote sensing of primary production. Int J Remote Sens. 7(11): 1395–1416.

Wall L, Larocque D, Léger PM. 2008. The early explanatory power of NDVI in crop yield modelling. Int J Remote Sens. 29(8):2211–2225.

Wang J, Rich PM, Price KP. 2003. Temporal responses of NDVI to precipitation and temperature in the central Great Plains, USA. Int J Remote Sens. 24(11):2345–2364.

Yamanura RM, Patil B. 2021. NDVI derived LAI model: a novel tool for crop monitoring. J Crop Weed. 17(1):76–85.

Zhang J, Huang Y, Yuan L, Yang G, Chen L, Zhao C. 2016. Using satellite multispectral imagery for damage mapping of armyworm (*Spodoptera frugiperda*) in maize at a regional scale. Pest Manag Sci. 72(2): 335–348.